JVI Journals.ASM.org

Comparison of Varicella-Zoster Virus RNA Sequences in Human Neurons and Fibroblasts

Nicholas L. Baird,[a] Jacqueline L. Bowlin,[a] Randall J. Cohrs,[a,b] Don Gilden,[a,b] Kenneth L. Jones[c]

Departments of Neurology,[a] Microbiology,[b] and Biochemistry & Molecular Genetics,[c] University of Colorado School of Medicine, Aurora, Colorado, USA

Varicella-zoster virus (VZV) infection causes varicella, after which the virus becomes latent in ganglionic neurons. In tissue culture, VZV-infected human neurons remain viable at 2 weeks, whereas fibroblasts develop cytopathology. Next-generation RNA sequencing was used to compare VZV transcriptomes in neurons and fibroblasts and identified only 12 differentially transcribed genes of the 70 annotated VZV open reading frames (ORFs), suggesting that defective virus transcription does not account for the lack of cell death in VZV-infected neurons *in vitro*.

Varicella-zoster virus (VZV) is an exclusively human neurotropic alphaherpesvirus that usually produces varicella (chickenpox) upon primary infection, after which the virus becomes latent in ganglionic neurons along the entire neuraxis. In tissue culture, VZV-infected neurons remain viable 2 weeks after infection, while all nonneuronal cells develop a cytopathic effect (CPE). Our earlier studies of VZV-infected neurons derived from induced pluripotent stem (iPS) cells revealed that neurons appeared healthy 2 weeks later, with no detectable infectious virus in the tissue culture medium; analysis of the neurons revealed VZV DNA, transcripts, and proteins corresponding to the VZV immediate early, early, and late kinetic phases of replication (1). Furthermore, ultrastructural examination revealed few complete virions and numerous aberrant viral particles (2). Together, these findings indicate that VZV is not latent in these neurons, despite the lack of CPE, and suggest a deficiency in replication and viral assembly in neurons during the productive infection. Thus, next-generation RNA sequencing (NextGen RNA-seq) was used to examine all annotated VZV transcripts in both cell types.

Terminally differentiated human neurons derived from human-induced pluripotent stem cells (iCell; Cellular Dynamics International, Madison, WI) and human fetal lung (HFL) fibroblasts were infected at a multiplicity of infection (MOI) of 1×10^{-3} cell-free vOka strain VZ virions (Zostavax; Merck, Whitehouse Station, NJ) as described previously (2). Total RNA was extracted from VZV-infected fibroblasts when ~80% CPE was reached and from VZV-infected neurons 14 days postinfection (dpi), at which time 5 to 10% of the neurons were infected. cDNA libraries were constructed for each sample (3 neuron, 3 fibroblast samples) using the Illumina TruSeq stranded-mRNA sample preparation kit (Illumina, San Diego, CA). The six independently and uniquely indexed libraries were pooled and loaded onto a single lane of a HiSeq2000 flow cell for paired-end, 100-bp DNA sequencing using an Illumina HiSeq2000.

NextGen RNA-seq of six cDNA libraries yielded 29.2 to 76.8 million total reads per sample (Fig. 1A). Removal of low-quality

Received 14 February 2014 **Accepted** 28 February 2014
Published ahead of print 5 March 2014
Editor: L. Hutt-Fletcher
Address correspondence to Don Gilden, don.gilden@ucdenver.edu.

doi:10.1128/JVI.00476-14

A

	total sequences (cell and VZV)	sequences after trimming (% total reads)	VZV-specific sequences (% total reads)	
			top strand	bottom strand
fibroblast-1	56,098,784	54,696,336 (98%)	3,509,090 (6%)	5,918,718 (11%)
fibroblast-2	75,395,136	73,478,014 (98%)	8,386,078 (11%)	13,019,180 (17%)
fibroblast-3	64,064,102	62,463,176 (98%)	4,751,610 (7%)	7,749,498 (12%)
neuron-1	44,179,892	43,092,966 (98%)	1,226,920 (3%)	1,876,620 (4%)
neuron-2	76,790,106	74,820,284 (97%)	1,720,426 (2%)	2,623,772 (3%)
neuron-3	29,164,536	28,655,270 (98%)	348,380 (1%)	535,910 (2%)

B

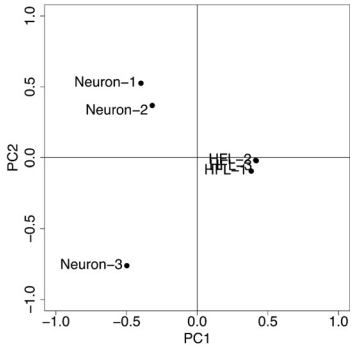

FIG 1 Analysis of NextGen RNA-seq data quality. (A) Quantification of viral transcripts identified by RNA-seq from VZV-infected fibroblasts and human neurons. (B) Variance among all six samples was analyzed. FPKMs from all libraries were separated using principal-component analysis (PCA). Principal component 1 (PC1) separated samples by their largest variance and resulted in separation between cell types. PC2 separated samples by the next-largest variance, independent of the first, and resulted in separation of samples within cell types. PCA analysis indicated a lack of variation between all three fibroblast samples, whereas neuron 3 was different from neurons 1 and 2. PCA analysis showed that neuron 3 was an outlier.

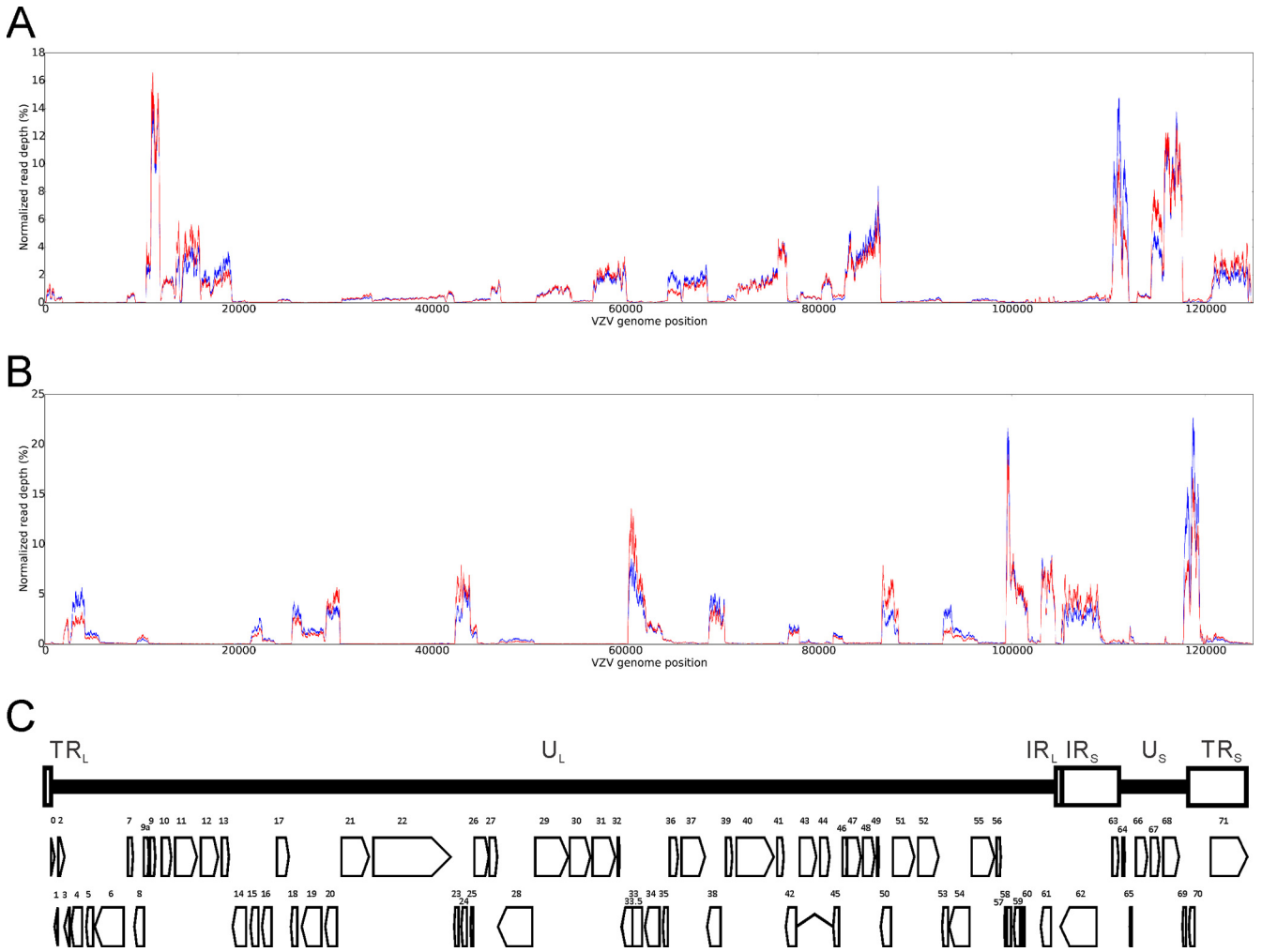

FIG 2 Normalized average read depths per base. The total number of times that each nucleotide was sequenced (raw DNA read depth) was normalized to the sum of numbers of all VZV transcripts in neurons (blue) and fibroblasts (red). Sequence reads were plotted for the top (A) or bottom (B) strands of the VZV genome. (C) Positions of both viral ORFs and physical features of VZV DNA. U_L and U_S, unique long and short sequences, respectively; TR_L and TR_S, terminal repeats of U_L and U_S, respectively; IR_L and IR_S, internal repeats of U_L and U_S, respectively.

bases (Phred score $<$ 15 [3, 4]) using a custom Python script reduced total sequence data by ≤4%. The remaining sequences were mapped to the annotated VZV genome (Dumas; NCBI accession number NC_001348) using GSNAP (Genomic Short-Read Nucleotide Alignment Program) (5). Viral sequences comprised 3 to 7% of all reads from VZV-infected neurons and 17 to 29% of reads from VZV-infected fibroblasts. The bidirectional, strand-specific cDNA library construction protocol permitted alignment of sequences to either the annotated Dumas strain (top strand) or the complementary (bottom) strand (Fig. 1A) of the VZV genome using Cufflinks (6). After strand alignment of VZV sequences, the number of fragments per kilobase of exon per million mapped reads (FPKM; a relative expression level normalized to the sum of all viral sequences divided by specific open reading frame [ORF] length) was determined. FPKMs from all six libraries were analyzed using the statistical transformation technique of principal-component analysis (PCA) to visualize the differences between samples (Fig. 1B). Samples were first separated by the largest component of variance (principal component 1 [PC1]) and then by the next-largest and independent component of variance (PC2). Based on PCA results and the low number of reads from neuron 3, it was considered to be an outlier and removed from further analysis.

After mapping of the five remaining libraries (two neuron, three fibroblast libraries), the average read depth per nucleotide was normalized to the total number of reads across the entire virus genome for each sample; read depths were averaged for all neuron (Fig. 2, blue) or all fibroblast (Fig. 2, red) samples and plotted by top (Fig. 2A) and bottom (Fig. 2B) strands. Figure 2C shows the relative locations of all annotated VZV ORFs and the directions of transcription.

VZV ORFs that were transcribed differently in neurons than in fibroblasts were identified based on their calculated fold changes in FPKMs and then by analysis of variance (ANOVA) using a two-neuron- by three-fibroblast-library design (Fig. 3A). Alignment of the fold changes in transcript levels from highest (greater transcription in neurons) to lowest (greater transcription in fibroblasts) revealed a break at a ±1.70-fold change (Fig. 3B, dotted horizontal lines). Based on a P value of ≤0.05 and a ±1.70-fold change, transcription of eight VZV ORFs was increased in neurons compared to in fibroblasts, and four VZV ORFs were transcribed less in neurons than in fibroblasts (Fig. 3A, asterisks).

A

VZV ORF	fibroblast mean[a]	neuron mean[b]	fold change[c]	P-value[d]	Q-value[e]	VZV ORF	fibroblast mean[a]	neuron mean[b]	fold change[c]	P-value[d]	Q-value[e]
0	9,398	6,045	-1.55	0.008	0.033	35	3,681	3,742	1.02	0.759	0.782
1	1,628	2,258	1.39	0.060	0.078	36*	6,994	15,260	2.18	<0.001	0.009
2	2,876	3,389	1.18	0.061	0.096	37	11,735	15,412	1.31	0.010	0.033
3	16,199	16,766	1.04	0.630	0.670	38	24,720	33,647	1.36	0.001	0.004
4*	23,122	40,570	1.75	0.022	0.033	39*	2,178	3,967	1.82	<0.001	0.006
5	6,094	9,615	1.58	0.006	0.016	40	11,390	12,138	1.07	0.194	0.229
6	1,186	1,631	1.38	0.020	0.030	41	31,635	32,977	1.04	0.172	0.216
7	5,205	4,536	-1.15	0.021	0.042	42/45[g]	8,374	11,005	1.31	0.008	0.018
8*	6,162	3,619	-1.70	0.002	0.008	43	3,506	3,593	1.02	0.787	0.808
9A	27,814	23,379	-1.19	0.209	0.240	44	13,785	12,900	-1.07	0.112	0.161
9	115,004	109,021	-1.05	0.141	0.188	46	22,843	26,643	1.17	0.053	0.089
10	13,110	13,582	1.04	0.023	0.043	47	24,580	28,132	1.14	0.033	0.059
11	32,013	22,211	-1.44	0.002	0.017	48	35,968	42,045	1.17	0.062	0.096
12	10,938	14,668	1.34	0.016	0.036	49	52,404	67,035	1.28	0.020	0.042
13	17,977	26,514	1.47	0.003	0.022	50*	51,531	26,915	-1.91	<0.001	0.001
14	391	345	-1.14	0.605	0.664	51	508	630	1.24	0.186	0.227
15	9,662	15,354	1.59	0.019	0.030	52	1,282	1,979	1.54	0.011	0.033
16	3,128	4,314	1.38	0.011	0.020	53*	12,354	29,437	2.38	0.002	0.008
17	1,531	1,876	1.23	0.015	0.036	54*	6,111	10,826	1.77	<0.001	0.001
18	23,051	31,500	1.37	0.008	0.018	55	1,203	1,896	1.58	0.003	0.022
19	9,326	12,165	1.30	0.050	0.071	56	809	563	-1.44	0.144	0.188
20	38,794	30,110	-1.29	0.002	0.008	57	117,743	154,076	1.31	0.087	0.105
21	3,276	2,412	-1.36	0.005	0.023	58	81,190	83,494	1.03	0.338	0.397
22	2,769	2,893	1.04	0.313	0.339	59	49,416	48,622	-1.02	0.783	0.783
23*	51,302	28,395	-1.81	0.001	0.004	60	34,475	32,633	-1.06	<0.001	0.001
24	55,348	47,793	-1.16	0.010	0.019	61	56,166	58,557	1.04	0.462	0.523
25	12,826	8,474	-1.51	<0.001	0.001	62/71	37,799	25,722	-1.47	0.052	0.071
26	1,835	2,318	1.26	0.005	0.023	62/71	22,037	15,987	-1.38	0.082	0.123
27	9,303	8,503	-1.09	0.017	0.036	63/70	106,381	149,985	1.41	0.005	0.015
28*	2,114	3,779	1.79	0.012	0.020	63/70	62,170	93,415	1.50	0.011	0.033
29	7,137	7,128	n/c[f]	0.891	0.891	64/69*	60,705	114,116	1.88	0.007	0.016
30	1,823	1,772	-1.03	0.488	0.514	64/69*	35,671	71,250	2.00	0.010	0.033
31	17,808	15,024	-1.19	0.015	0.036	65*	3,658	6,894	1.88	0.005	0.015
32	26,353	21,745	-1.21	0.012	0.035	66	3,811	4,460	1.17	0.130	0.182
33	56,724	41,271	-1.37	0.010	0.019	67	57,005	36,734	-1.55	0.002	0.017
33.5*	39,474	22,941	-1.72	<0.001	0.001	68	85,844	87,358	1.02	0.258	0.288
34	15,662	14,505	-1.08	0.081	0.102						

[a] Average FPKM from three independent samples. [b] Average FPKM from two independent samples. [c] Fold-change of neuron FPKM relative to fibroblast FPKM. [d] Significance value from ANOVA comparisons of neuron FPKM relative to fibroblast FPKM. [e] Bonferroni adjusted p-value. [f] No change to two significant figures. [g] ORFs 42 and 45 are a single spliced transcript. * ORFs which were expressed greater than or equal to ±1.7 fold in neurons compared to fibroblasts.

B

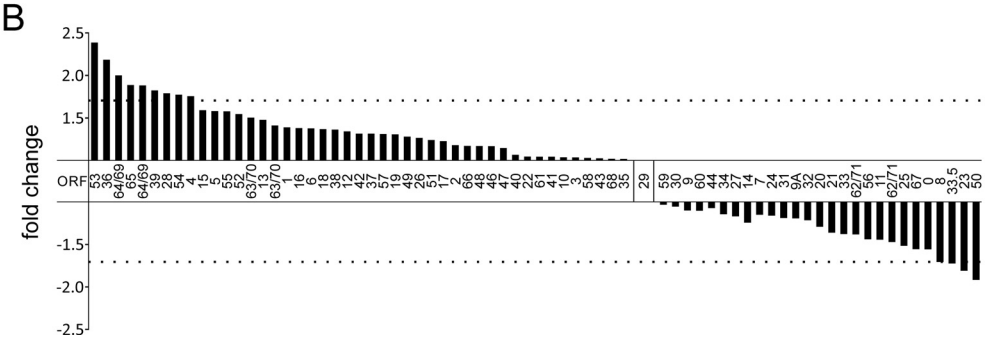

FIG 3 Fold changes in numbers of VZV transcripts in human neurons from their numbers in fibroblasts. (A) ANOVA of VZV transcript numbers from VZV-infected fibroblasts and human neurons. (B) Fold changes in the numbers of VZV transcripts for all ORFs in infected human neurons from those in fibroblasts, arranged from highest (greater in neurons) to lowest (greater in fibroblasts). Dotted horizontal lines denote a ±1.70-fold change in transcript levels between cell types. ORFs 53, 36, 64/69, 65, 39, 28, 54, and 4 were transcribed more in neurons, and ORFs 50, 23, 33.5, and 8 were transcribed more in fibroblasts.

To validate NextGen RNA-seq results, reverse transcription quantitative PCR (RT-qPCR) was performed on five differentially transcribed VZV ORFs as described previously (7) using the same RNAs used for RNA-seq. VZV ORF 53, 54, and 64/69 transcripts were more abundant in neurons than in fibroblasts, while VZV ORF 23 and 50 transcripts were more abundant in fibroblasts (Fig. 3B). Since RNA-seq data were normalized to total VZV transcript levels (FPKM), each RT-qPCR also required normalization. For this, VZV ORF 29 was used since the ratio of the level of this transcript in virus-infected neurons to its level in fibroblasts was 1 (i.e., the transcript abundances did not differ between cell types) (Fig. 3). After normalization, the fold change of the level of transcription of each VZV ORF in infected neurons from the level of transcription in infected fibroblasts was determined (Fig. 4A,

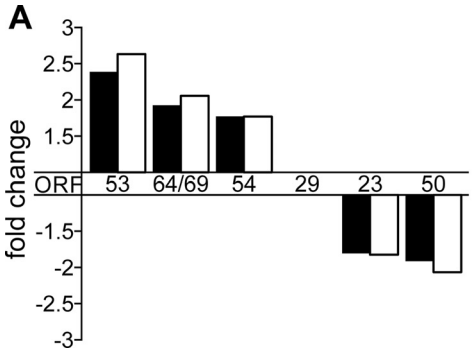

B

VZV ORF	RNAseq fibroblast	RNAseq neuron	RT-qPCR fibroblast	RT-qPCR neuron
23	51,302	28,394	295,757	50,064
29	7,136	7,127	27,357	8,446
50	51,531	26,914	371,300	55,515
53	12,353	29,437	58,085	47,199
54	6,111	10,825	1,572	857
64/69[a]	48,188	92,682	271,792	172,373

[a] Average FPKM from RNAseq of both copies of the repeated sequence for ORFs 64/69

FIG 4 Validation of RNA-seq by RT-qPCR. RNA used in RNA-seq analysis was reverse transcribed with oligo(dT), and primers and cDNA were analyzed by RT-qPCR. Primer/probe sets were designed for five VZV ORFS that exceeded the ±1.70-fold cutoff; three genes (ORFs 53, 64/69, and 54) were transcribed more in neurons, and two genes (ORFs 23 and 50) were transcribed less in neurons. Each RT-qPCR mixture contained a primer/probe set for ORF 29 for normalization. (A) Fold changes (from neurons to fibroblasts) in the levels of transcription of the six ORFs from RNA-seq analysis (black bars) or by RT-qPCR after normalization to ORF 29 (white bars). (B) Raw data from RNA-seq (FPKMs) and RT-qPCR (copy numbers) used to construct the graph in panel A.

white bars). RT-qPCR results were the same as those found using NextGen RNA-seq technology (Fig. 4A, black bars).

Herein, next-generation RNA sequencing was used to better understand the absence of CPE during productive VZV infection of human neurons compared to the effects of infection of fibroblasts by determining the complete virus transcriptome in each cell type. Surprisingly, only 12 of the 70 VZV ORFs showed differences in transcript abundance between the two cell types.

We found that VZV-infected human neurons in cell culture transcribed every annotated ORF, unlike the limited viral transcription present in human and monkey ganglia latently infected with varicella-zoster virus (8–10). This confirmed a significant difference in virus gene transcription *in vitro* from that in human neurons latently infected with VZV. A comparison of the 12 differentially transcribed VZV ORFs to orthologous herpes simplex virus 1 (HSV-1) genes revealed that they did not belong to a unique class of virus genes: one was immediate early (ORF 4), three were early (ORFs 8, 28, and 36), and eight were late (ORFs 23, 33.5, 39, 50, 53, 54, 64/69, and 65); six were essential (ORFs 4, 28, 33.5, 39, 53, and 54) and six were nonessential (ORFs 8, 23, 36, 50, 64/69, and 65); and nine mapped to the bottom strand (ORFs 4, 8, 23, 28, 33.5, 50, 53, 54 and 65), two to the top strand (ORFs 36 and 39), and one to both strands (ORF 64/69). Overall, viral transcription in neurons that survive 2 weeks after VZV infection does not appear to be defective compared to that in fibroblasts. Further studies are needed to compare the rates of VZV DNA replication in neurons and fibroblasts.

ACKNOWLEDGMENTS

This work was supported by Public Health Service grants AG006127 (D.G.), AG032958 (D.G. and R.J.C.), and NS082228 (R.J.C.) from the National Institutes of Health. N. L. Baird was supported by training grant NS007321 to D. Gilden from the National Institutes of Health. K. L. Jones and RNA sequencing were supported in part by the Genomics and Biostatistics/Bioinformatics Shared Resources of Colorado's NIH/NCI Cancer Center (support grant P30CA046934).

We thank Marina Hoffman for editorial review and Lori DePriest for manuscript preparation.

REFERENCES

1. **Yu X, Seitz S, Pointon T, Bowlin JL, Cohrs RJ, Jonjic S, Haas J, Wellish M, Gilden D.** 2013. Varicella zoster virus infection of highly pure terminally differentiated human neurons. J. Neurovirol. **19:**75–81. http://dx.doi.org/10.1007/s13365-012-0142-x.
2. **Grose C, Yu X, Cohrs RJ, Carpenter JE, Bowlin JL, Gilden D.** 2013. Aberrant virion assembly and limited glycoprotein C production in varicella-zoster virus-infected neurons. J. Virol. **87:**9643–9648. http://dx.doi.org/10.1128/JVI.01506-13.
3. **Ewing B, Green P.** 1998. Base-calling of automated sequencer traces using phred. II. Error probabilities. Genome Res. **8:**186–194.
4. **Ewing B, Hillier L, Wendl MC, Green P.** 1998. Base-calling of automated sequencer traces using phred. I. Accuracy assessment. Genome Res. **8:**175–185.
5. **Wu TD, Nacu S.** 2010. Fast and SNP-tolerant detection of complex variants and splicing in short reads. Bioinformatics **26:**873–881. http://dx.doi.org/10.1093/bioinformatics/btq057.
6. **Trapnell C, Hendrickson DG, Sauvageau M, Goff L, Rinn JL, Pachter L.** 2013. Differential analysis of gene regulation at transcript resolution with RNA-seq. Nat. Biotechnol. **31:**46–53. http://dx.doi.org/10.1038/nbt.2450.
7. **Cohrs RJ, Gilden DH.** 2007. Prevalence and abundance of latently transcribed varicella-zoster virus genes in human ganglia. J. Virol. **81:**2950–2956. http://dx.doi.org/10.1128/JVI.02745-06.
8. **Meyer C, Kerns A, Barron A, Kreklywich C, Streblow DN, Messaoudi I.** 2011. Simian varicella virus gene expression during acute and latent infection of rhesus macaques. J. Neurovirol. **17:**600–612. http://dx.doi.org/10.1007/s13365-011-0057-y.
9. **Nagel MA, Choe A, Traktinskiy I, Cordery-Cotter R, Gilden D, Cohrs RJ.** 2011. Varicella-zoster virus transcriptome in latently infected human ganglia. J. Virol. **85:**2276–2287. http://dx.doi.org/10.1128/JVI.01862-10.
10. **Ouwendijk WJ, Choe A, Nagel MA, Gilden D, Osterhaus AD, Cohrs RJ, Verjans GM.** 2012. Restricted varicella-zoster virus transcription in human trigeminal ganglia obtained soon after death. J. Virol. **86:**10203–10206. http://dx.doi.org/10.1128/JVI.01331-12.